optica

Spatio-temporal imaging of light transport in highly scattering media under white light illumination: supplementary material

AMAURY BADON, DAYAN LI, GEOFFROY LEROSEY, A . CLAUDE BOCCARA, MATHIAS FINK, AND ALEXANDRE AUBRY*

Institut Langevin, ESPCI ParisTech, PSL Research University, CNRS UMR 7587, 1 rue Jussieu, 75005 Paris, France
**Corresponding author: alexandre.aubry@espci.fr*

Published 24 October 2016

This document provides supplementary information to "Spatio-temporal imaging of light transport in highly scattering media under white light illumination," http://dx.doi.org/10.1364/optica.3.001160. The information is on the convergence of the time derivative of the mutual coherence function towards the Green's functions, the measurement of the diffusion constant components in isotropic and anisotropic scattering media and its comparison with a time-of-flight experiment.

http://dx.doi.org/10.1364/optica.3.001160.s001

1. CONVERGENCE OF THE TIME DERIVATIVE OF THE MUTUAL COHERENCE FUNCTION

The passive measurement of the Green's function is based on the fundamental property that the time derivative of the correlation function should converge for infinite integration times towards the difference between the causal and anti-causal Green's functions [see Eq.1 of the accompanying paper]. In practice, this integration time remains fixed to $T = 750$ ms in the experiments shown in the accompanying paper. Hence the measured signal may be polluted by noise. To assess the signal-to-noise ratio (SNR) in our measurements, the convergence of $\partial_t C$ as a function of the integration time T should be investigated. It can be expressed as the sum of a deterministic term that resists to average, the expected Green's functions, and a noise term that should vanish with average

$$\partial_t C(t) = \underbrace{\{g(t) - g(-t)\}}_{\text{signal}} + \underbrace{\frac{1}{T}\int_0^T n(\tau)d\tau}_{\text{noise}} \qquad \textbf{(S1)}$$

where $n(\tau)$ accounts for the incoherent noise term whose coherence time τ_c is governed by the bandwidth of the white light source. To estimate the SNR, the mean intensity of Eq.S1 should be considered. It yields

$$\left\langle |\partial_t C|^2 \right\rangle = \underbrace{\left\langle |\{g(t) - g(-t)\}|^2 \right\rangle}_{\text{signal intensity}} + \underbrace{\frac{1}{T^2}\left|\left\langle \int_0^T n(\tau)d\tau \right\rangle\right|^2}_{\text{noise intensity}} \qquad \textbf{(S2)}$$

The coherence properties of the noise $n(\tau)$ allows to simplify the last equation into

$$\left\langle |\partial_t C|^2 \right\rangle = \underbrace{\left\langle |\{g(t) - g(-t)\}|^2 \right\rangle}_{\text{signal intensity}} + \underbrace{\frac{\tau_c}{T}\left\langle |n(\tau)|^2 \right\rangle}_{\text{noise intensity}} \qquad \textbf{(S3)}$$

Not surprisingly, the noise intensity should decrease as the inverse of the integration time T. Fig.S1 confirms this behavior by showing the spatially averaged intensity of $\partial_t C(t)$ measured in the TiO_2 layer as a function of T. For short time delays ($\delta = 0$ μm in Fig.S1), the signal intensity is sufficiently large to make the convergence of $\partial_t C(t)$ nearly immediate. For intermediate time delays ($\delta = 20 - 100$ μm in Fig.S1), $\left\langle |\partial_t C|^2 \right\rangle$ decreases as $1/T$ for small integration times before saturating at the signal level for large integration times. This means that the integration time $T = 750$ ms is enough to get rid of most of the noise background and have a satisfying estimation of the Green's function. On the contrary, for larger time delays ($\delta = 130$ μm in Fig.S1), the signal intensity is too weak to emerge from the noise background: $\left\langle |\partial_t C|^2 \right\rangle$ decreases as $1/T$ over the whole integration

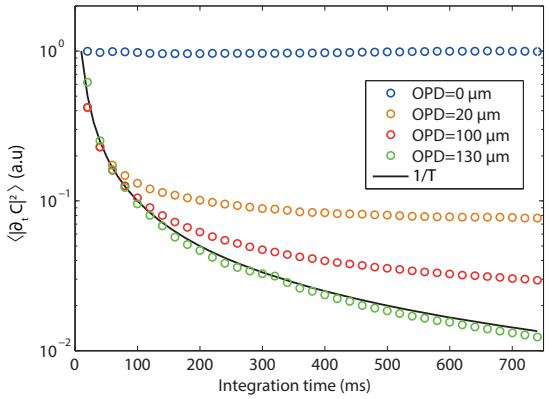

Fig. S1. Convergence of the time derivative of the mutual coherence function in the TiO_2 layer. The spatially averaged intensity of the mutiual coherence functoin, $\langle|\partial_t C|^2\rangle$, is plotted as a function of the integration time T at different OPDs. The continous black line shows for comparison the expected noise intensity decrease as $1/T$ (see Eq.S3).

time range, which is characteristic of a predominant noise background. The value of $\langle|\partial_t C|^2\rangle$ at time $T = 750$ ms allows to determine the noise level in our experiment. A SNR can be derived for each OPD: SNR$\sim 10^2$ at $\delta = 0$ μm, SNR~ 8 at $\delta = 20$ μm and SNR~ 3 at $\delta = 100$ μm. Note that this noise background is systematically subtracted from the raw mean intensity prior to investigating the growth of the diffusive halo in each experiment.

2. INCOHERENT INTENSITY IN THE MULTIPLE SCATTERING REGIME

In this section we investigate the case of the propagation of light in the multiple scattering regime. As mentioned in the article, the energy density W whose flux corresponds to the incoherent intensity obeys the diffusion equation :

$$\frac{\partial W(\mathbf{r},t)}{\partial t} = D\Delta W(\mathbf{r},t) - \frac{c}{l_a}W(\mathbf{r},t) + S(\mathbf{r},t). \qquad \textbf{(S4)}$$

with $S(\mathbf{r},t)$ a source function, l_a the absorption mean free path and D the diffusion constant. The solution of this equation corresponds to a diffusive halo whose spatial extent broadens with time [see Fig. S2]. Its mathematical expression also depends on the boundary conditions. In the accompanying paper, the samples under study consist in strongly scattering layers of thickness $L \sim 80$ μm. The characteristic time for the diffusive wavefield to travel through the scattering medium is given by the Thouless time $\tau_D = L^2/D \sim 6$ ps for $D = 730$ m^2/s. As the temporal range investigated in our study is of the order of 500 fs, the scattering medium can thus be considered as semi-infinite. In these conditions, *Patterson et al.* [1] established the expression for the backscattered incoherent intensity :

$$I_{inc}(\Delta r,t) = (4\pi D)^{-3/2} z_0 t^{-5/2} \exp\left(-\frac{ct}{l_a}\right)\exp\left(-\frac{\Delta r^2}{4Dt}\right) \qquad \textbf{(S5)}$$

with z_0 the extrapolation length [2] and Δr the source-receiver distance. The incoherent intensity can thus be written as the

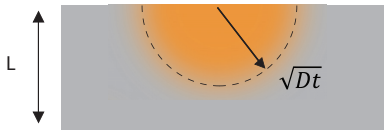

Fig. S2. Expansion of the diffusive halo in a scattering slab

product of two terms:

$$I_{inc}(\Delta r,t) = I_z(t)\exp\left(-\frac{\Delta r^2}{4Dt}\right) \qquad \textbf{(S6)}$$

with :

$$I_z(t) = (4\pi D)^{-3/2} z_0 t^{-5/2} \exp\left(-\frac{ct}{l_a}\right) \qquad \textbf{(S7)}$$

The first term $I_z(t)$ accounts for the temporal decreasing of the incoherent intensity whereas the second term in $\exp(-\Delta r^2/4Dt)$ accounts for the temporal growth of the diffusive halo. By normalizing the incoherent intensity at each time flight, one can therefore investigate the the diffusive properties of the scattering medium independently from the absorption losses.

3. INCOHERENT INTENSITY FOR AN ANISOTROPIC SCATTERING MEDIUM

In this section, we investigate the case of the propagation of light in an anisotropic scattering medium. In such a medium, the diffusion equation is now given by [3]:

$$\frac{\partial W(\mathbf{r},t)}{\partial t} = \nabla.\mathbf{D}\nabla W(\mathbf{r},t) - \frac{c}{l_a}W(\mathbf{r},t) + S(\mathbf{r},t). \qquad \textbf{(S8)}$$

with $W(\mathbf{r},t)$ the energy density, $S(\mathbf{r},t)$ a source function, l_a the absorption mean free path and $\mathbf{D}$ the diffusion tensor. According to Ref.[4], the corresponding incoherent intensity is given by:

$$I(\Delta x,\Delta y,t) = I_z(t)\exp\left(-\frac{\Delta x^2}{D_{xx}}\right)\exp\left(-\frac{\Delta y^2}{D_{yy}}\right). \qquad \textbf{(S9)}$$

with D_{xx} and D_{yy} the in-plane components of the diffusion tensor. Δx and Δy are the projections of the source-receiver relative positions along the x and y-axis. For a semi-infinite medium, I_z is given by:

$$I_z(t) = \left(D_{xx}D_{yy}D_{zz}\right)^{-1/2} z_0 t^{5/2} \exp\left(-\frac{ct}{l_a}\right). \qquad \textbf{(S10)}$$

At a given time of flight, the normalized incoherent intensity can be expressed as:

$$\frac{I_{inc}(\Delta x,\Delta y,t)}{I_{inc}(0,0,t)} = \exp\left(-\frac{\Delta x^2}{4D_{xx}t}\right)\exp\left(-\frac{\Delta y^2}{4D_{yy}t}\right) \qquad \textbf{(S11)}$$

As in the isotropic case, the normalized incoherent intensity is independent on the absorption losses.

Fig. S3 displays the spatio-temporal evolution of the mean intensity measured in the stretched Teflon tape. The two components D_{xx} and D_{yy} of the diffusion tensor can be estimated separately. First, the relative position Δx is set to 0 and the mean intensity is investigated as a function of time and Δy [see Fig. S3(b)]. A linear fit of the square width W^2 of the diffusive halo versus time allows an estimation of D_{yy}=3000 m^2.s^{-1}. Alternatively, by setting $\Delta y = 0$, we can investigate the diffuse intensity as a function of time and Δx [see Fig.S3(d)]. Again, a linear fit of W^2 yields an estimation of D_{xx}=1100 m^2.s^{-1}.

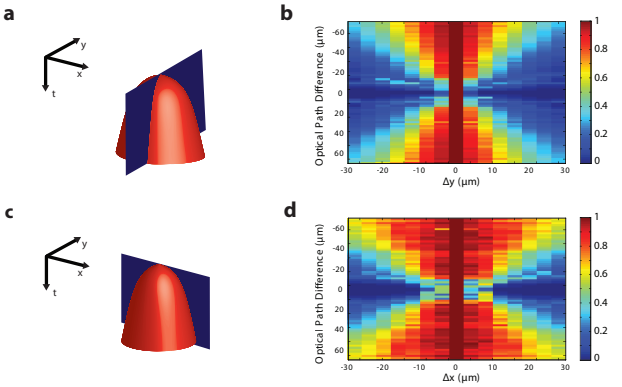

Fig. S3. Anisotropic diffusion in a stretched Teflon tape. (a) Sketch of the spatio-temporal diffusive halo and its section at $\Delta x = 0$. (b) Measured spatio-temporal evolution of the mean intensity at $\Delta x = 0$. The intensity is renormalized by its maximum at each time of flight. (c) Sketch of the spatio-temporal evolution of the mean intensity and its section at $\Delta y = 0$. (d) Measured spatio-temporal evolution of the mean intensity for $\Delta y = 0$. The intensity is renormalized by its maximum at each time of flight.

4. TIME-OF-FLIGHT DISTRIBUTION IN THE TiO_2 LAYER

In this section, we investigate the time-of-flight distribution of the reflected intensity integrated over the surface of the scattering sample,

$$R(t) = \int I(\Delta \mathbf{r}, t) d^2 \Delta \mathbf{r}. \qquad \textbf{(S12)}$$

The decay of the reflected intensity with time bears particular signatures of light diffusion. For times of flight smaller than the Thouless time τ_D, the medium can be considered as semi-infinite. In that case, a power law decay is expected for the reflected intensity at the surface of the sample [5]:

$$R(t) \propto t^{-3/2}. \qquad \textbf{(S13)}$$

At longer times of flight, the finite sample size should come into play so that the decay becomes similar to that of time-dependent transmission, i.e., exponential in the diffuse regime [5, 6], such that

$$R(t) \propto \exp\left(-\frac{ct}{l_a}\right) \exp\left(-\frac{\pi^2 D t}{(L+2z_o)^2}\right) \qquad \textbf{(S14)}$$

In absence of absorption ($l_a \rightarrow \infty$), the time-of-flight distribution of the backscattered intensity is thus an alternative way of measuring the diffusion constant D.

An experimental set up involving a coherent illumination scheme and an interferometric arm in reception [7] has been used to measure $R(t)$ in the TiO_2 layer over an extensive range of time-of-flight. The result is displayed in Fig.S4. As predicted by theory [Eq.S13], the experimental time-of-flight distribution can be qualitatively fitted by the $t^{-3/2}$ power law for $t << \tau_D$ [see Fig.S4(a)]. In agreement with theory, the time decay of $R(t)$ becomes exponential at larger times of flight [see Fig.S4(b)]. If we neglected absorption losses, a fit of the exponential decay would yield an estimation of the diffusion constant $D \sim 1250$ $m^2.s^{-1}$. This value is quite far from our measurement deduced with the growth of the diffusive halo ($D \simeq 730\ m^2.s^{-1}$, see Sec.3A of the accompanying paper). The mismatch between

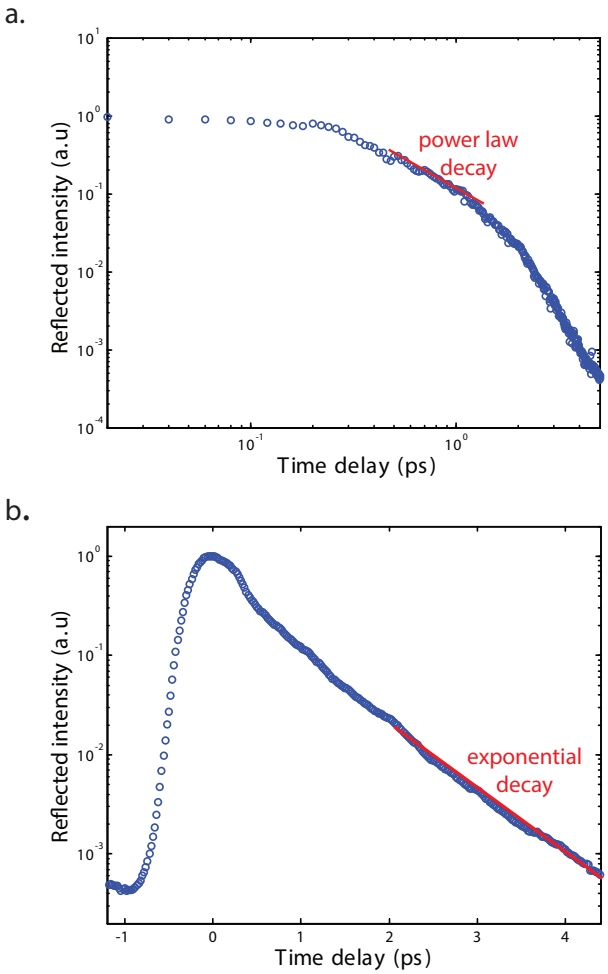

Fig. S4. Time-of-flight distribution of the intensity reflected by the TiO_2 sample. (a) The time-evolution of $R(t)$ (blue circles) is plotted in a log-log scale and fitted with the $t^{-3/2}$ power law over the time range [500 fs - 1 ps]. (b) The time-evolution of $R(t)$ (blue circles) is plotted in a linear-log scale and fitted with an exponential decay over the time range [2 ps - 4.5 ps].

both values can be easily accounted for by the presence of absorption losses. Considering that $D \simeq 730\ m^2.s^{-1}$, the exponential decay fit performed in Fig.S4(b) leads to the following estimation for the absorption mean free path: $l_a \simeq 118\ \mu$m. This time-of-flight experiment illustrates the benefit of our approach that allows a quantitative measurement of the diffusion constant, independent from the absorption losses.

REFERENCES

1. M. S. Patterson, B. Chance, and B. C. Wilson, "Time resolved reflectance and transmittance for the noninvasive measurement of tissue optical properties," Appl. Opt. **28**, 2331–2336 (1989).
2. D. J. Durian, "Influence of boundary reflection and refraction on diffusive photon transport," Phys. Rev. E **50**, 857–866 (1994).
3. D. S. Wiersma, A. Muzzi, M. Colocci, and R. Righini, "Time-

resolved experiments on light diffusion in anisotropic random media," Phys. Rev. E **62**, 6681–6687 (2000).
4. E. Simon, P. Krauter, and A. Kienle, "Time-resolved measurements of the optical properties of fibrous media using the anisotropic diffusion equation," J. Biomed Opt. **19**, 075006–075006 (2014).
5. P. M. Johnson, A. Imhof, B. P. J. Bret, J. G. Rivas, and A. Lagendijk, "Time-resolved pulse propagation in a strongly scattering material," Phys. Rev. E **68**, 016604 (2003).
6. J. H. Page, , H. P. Schriemer, A. E. Bailey, and D. A. Weitz, "Experimental test of the diffusion approximation for multiply scattered sound," Phys. Rev. E **52**, 3106–14 (1995).
7. A. Badon, D. Li, G. Lerosey, A. C. Boccara, M. Fink, and A. Aubry, "Smart optical coherence tomography for ultra-deep imaging through highly scattering media," arxiv:510.08613 (2015).